Short, Strong Hydrogen Bonds at the Active Site of Human Acetylcholinesterase: Proton NMR Studies[†]

Michael A. Massiah,[‡] Carol Viragh,[§] Putta M. Reddy,[§] Ildiko M. Kovach,*[,§] Joseph Johnson,[||] Terrone L. Rosenberry,[||] and Albert S. Mildvan*[,‡]

Department of Biological Chemistry, Johns Hopkins School of Medicine, Baltimore, Maryland 21205, Department of Chemistry, The Catholic University of America, Washington, D.C. 20064, and Department of Pharmacology, Mayo Foundation for Medical Education and Research, and Department of Research, Mayo Clinic Jacksonville, Jacksonville, Florida 32224

Received February 5, 2001; Revised Manuscript Received March 14, 2001

ABSTRACT: Cholinesterases use a Glu−His−Ser catalytic triad to enhance the nucleophilicity of the catalytic serine. We have previously shown by proton NMR that horse serum butyryl cholinesterase, like serine proteases, forms a short, strong hydrogen bond (SSHB) between the Glu−His pair upon binding mechanism-based inhibitors, which form tetrahedral adducts, analogous to the tetrahedral intermediates in catalysis [Viragh, C., et al. (2000) *Biochemistry 39*, 16200−16205]. We now extend these studies to human acetylcholinesterase, a 136 kDa homodimer. The free enzyme at pH 7.5 shows a proton resonance at 14.4 ppm assigned to an imidazole NH of the active-site histidine, but no deshielded proton resonances between 15 and 21 ppm. Addition of a 3-fold excess of the mechanism-based inhibitor *m*-(*N*,*N*,*N*-trimethylammonio)-trifluoroacetophenone (TMTFA) induced the complete loss of the 14.4 ppm signal and the appearance of a broad, deshielded resonance of equal intensity with a chemical shift δ of 17.8 ppm and a D/H fractionation factor ϕ of 0.76 ± 0.10, consistent with a SSHB between Glu and His of the catalytic triad. From an empirical correlation of δ with hydrogen bond lengths in small crystalline compounds, the length of this SSHB is 2.62 ± 0.02 Å, in agreement with the length of 2.63 ± 0.03 Å, independently obtained from ϕ. Upon addition of a 3-fold excess of the mechanism-based inhibitor 4-nitrophenyl diethyl phosphate (paraoxon) to the free enzyme at pH 7.5, and subsequent deethylation, two deshielded resonances of unequal intensity appeared at 16.6 and 15.5 ppm, consistent with SSHBs with lengths of 2.63 ± 0.02 and 2.65 ± 0.02 Å, respectively, suggesting conformational heterogeneity of the active-site histidine as a hydrogen bond donor to either Glu-327 of the catalytic triad or to Glu-199, also in the active site. Conformational heterogeneity was confirmed with the methylphosphonate ester anion adduct of the active-site serine, which showed two deshielded resonances of equal intensity at 16.5 and 15.8 ppm with ϕ values of 0.47 ± 0.10 and 0.49 ± 0.10 corresponding to average hydrogen bond lengths of 2.59 ± 0.04 and 2.61 ± 0.04 Å, respectively. Similarly, lowering the pH of the free enzyme to 5.1 to protonate the active-site histidine ($pK_a = 6.0 \pm 0.4$) resulted in the appearance of two deshielded resonances, at 17.7 and 16.4 ppm, consistent with SSHBs with lengths of 2.62 ± 0.02 and 2.63 ± 0.02 Å, respectively. The NMR-derived distances agree with those found in the X-ray structures of the homologous acetylcholinesterase from *Torpedo californica* complexed with TMTFA (2.66 ± 0.28 Å) and sarin (2.53 ± 0.26 Å) and at low pH (2.52 ± 0.25 Å). However, the order of magnitude greater precision of the NMR-derived distances establishes the presence of SSHBs at the active site of acetylcholinesterase, and detect conformational heterogeneity of the active-site histidine. We suggest that the high catalytic power of cholinesterases results in part from the formation of a SSHB between Glu and His of the catalytic triad.

With butyrylcholinesterase (BChE)[1] from horse serum, a 360 kDa homotetramer, we have recently reported the detection by NMR of a short, strong hydrogen bond (SSHB) between the Glu and His residues of the Glu−His−Ser catalytic triad (*1*). This SSHB was observed following covalent modification of the enzyme with mechanism-based inhibitors, which formed tetrahedral adducts of the catalytic serine analogous to the tetrahedral intermediates in catalysis.

[†] This work was supported by National Institutes of Health Grant DK 28616 (to A.S.M.) and by United States Army Medical Research and Material Command Contract DAMD17-98-8021 (to I.M.K.).

* To whom correspondence should be addressed. A.S.M.: phone, (410) 955-2038; fax, (410) 955-5759; e-mail, Mildvan@welchlink.welch.jhu.edu. I.M.K.: phone, (202) 319-6550; fax, (202) 319-5381; e-mail, Kovach@cua.edu.

[‡] Johns Hopkins School of Medicine.

[§] The Catholic University of America.

[||] Mayo Clinic Jacksonville.

[1] Abbreviations: AChE, acetylcholinesterase (acetyl hydrolase); ATC, acetylthiocholine; BChE, butyrylcholinesterase; Chelex-100, polystyrene divinylbenzene iminodiacetate sodium form; DIFP, diisopropyl fluorophosphate; DTNB, 5,5′-dithiobis(2-nitrobenzoic acid); NPMP, 4-nitrophenyl 2-propyl methylphosphonate; paraoxon, diethyl 4-nitrophenyl phosphate; sarin, 2-propylmethylphosphonofluoride; soman, 2-(3,3-dimethylbutyl)methylphosphonofluoridate; SSHB, short, strong hydrogen bond; TMTFA, *m*-(*N*,*N*,*N*-trimethylammonio)trifluoroacetophenone; TSP, 3-(trimethylsilyl)propionate-2,2,3,3-d_4; VX, *O*-ethyl-*S*-{2-[bis(1-methylethyl)amino]ethyl}methylphosphonothioate.

10.1021/bi010243j CCC: $20.00
Published on Web 04/21/2001

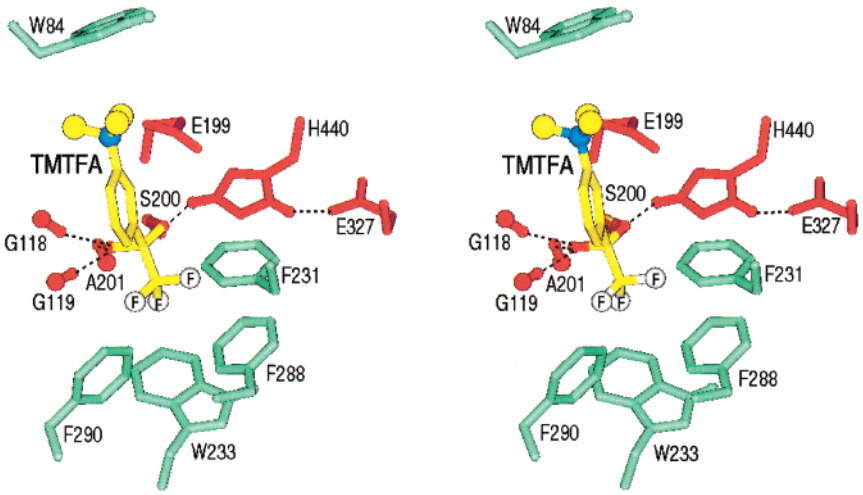

FIGURE 1: Stereopair showing the X-ray structure of the active site of *T. californica* AChE complexed with the mechanism-based inhibitor TMTFA (*21*). Hydrophobic residues are shown in green. Shown in red are the catalytic triad (Glu-327, His-440, and Ser-200), the oxyanion hole (Gly-118, Gly-119, and Ala-201), and Glu-199. The carboxylate of Glu-199 approaches both the tetramethylammonium group of TMTFA (3.5 Å) and the face of the imidazolium ring of His-440 at distances of 4.2 and 3.3 Å from Nδ and Nϵ, respectively. While close enough for van der Waals and electrostatic interactions, both the distances and angles are inappropriate for hydrogen bonding between Glu-199 and His-440 in this complex.

Deshielded proton resonances at 18.1 and 16.1 ppm appeared upon addition of *m*-(*N*,*N*,*N*-trimethylammonio)trifluoroacetophenone (TMTFA) and 4-nitrophenyl diethyl phosphate (paraoxon), respectively. From the chemical shifts and the low D/H fractionation factors of these resonances, hydrogen bond distances of 2.61 ± 0.03 and 2.63 ± 0.04 Å were calculated for the TMTFA and paraoxon adducts, respectively, establishing the presence of a SSHB at the active site of a serine esterase analogous to those previously found in serine proteases (*2*−*9*). For both proteases and esterases, which use serine nucleophiles, it was proposed that the SSHB between the carboxylate group and the NδH of the histidine in the catalytic triad increased the basicity of the histidine, permitting it to deprotonate the catalytic serine (*1*, *3*). Molecular dynamics simulations of acetylcholinesterase (AChE) from *Torpedo californica* suggested the shortening of the Glu to His distance upon the binding of mechanism-based inhibitors (*10*−*13*).

NMR criteria for the detection of SSHBs have been set forth (*9*, *14*), and have been applied to ketosteroid isomerase (*15*, *16*), triosephosphate isomerase (*17*), methylglyoxal synthase (*18*), serine proteases (*3*), and BChE (*1*). Briefly, the proton in a SSHB is highly deshielded, resulting in a low-field ^{1}H resonance between 15 and 19 ppm. The D/H fractionation factors of such protons are significantly lower than 1.0. Their solvent exchange rates are slowed by at least 1 order of magnitude, and their strengths are ≥5 kcal/mol (*9*, *14*). Further, the chemical shifts and fractionation factors of the protons in hydrogen bonds provide independent, precise, and accurate methods for measuring hydrogen bond lengths with errors of ≤0.05 Å (*1*, *9*, *14*).

In general, the presence of a SSHB cannot be established by protein X-ray diffraction because the errors in interatomic distances are 0.1−0.3 times the resolution, or ±0.2−0.6 Å for a typical 2 Å X-ray structure (*9*, *19*). These large errors preclude distinguishing between a SSHB 2.45−2.65 Å in length and a normal, weak hydrogen bond 2.75−3.00 Å in length (*9*). Thus, the X-ray structures of AChE from *T. californica* at low pH (*20*), and in a number of its complexes with mechanism-based inhibitors, which form tetrahedral serine adducts (Figure 1), show distances between Glu-327 Oϵ and His-440 Nδ of the catalytic triad which range from 2.52 ± 0.25 to 2.67 ± 0.23 Å (*21*−*23*). Although these distances may reflect the presence of a SSHB, the error ranges do not rule out a normal, weak hydrogen bond, ≥2.75 Å in length, as found in ice (*24*).

Scheme 1 illustrates a mechanism for cholinesterases showing the participation of SSHBs in the tetrahedral intermediates of the acylation and deacylation reactions of the catalytic serine (*1*, *25*). The SSHB forms when the catalytic His becomes protonated as a result of its deprotonation of the Ser (or water) nucleophile.

AChEs hydrolyze their natural substrate, acetylcholine, at low concentrations with a k_{cat}/K_m of 1.6×10^8 M^{-1} s^{-1} at 25 °C, pH 7.4, and an ionic strength (*I*) of 0.1 (*26*), approaching the diffusional rate limit at low ionic strength and viscosity (*27*, *28*), and with a k_{cat} of 1.6×10^4 s^{-1} at saturating substrate concentrations. Comparison of k_{cat} with the pseudo-first-order rate constant for the spontaneous hydrolysis of acetylcholine at the same temperature and pH reveals a rate acceleration or catalytic power of 10^{13}-fold (*27*, *28*), which is 10^3-fold greater than those of serine proteases. The high catalytic power of AChE, and of cholinesterases in general, may be attributed to their efficient use of the catalytic triad, the oxyanion hole, and at least two substrate binding regions or subsites (Figure 1). The X-ray structures of *T. californica* AChE indicate that the catalytic triad consists of Glu-327, His-440, and Ser-200 (*20*, *21*).[2] The oxyanion hole consists of the backbone NH groups of Gly-118, Gly-119, and Ala-201, three potential hydrogen bond donors rather than two as found in serine proteases. Phe-288, Phe-290, and Trp-233 are components of the acetyl-binding subsite; Glu-199 and Trp-84 contribute to the choline-binding subsite, and Phe-331 contributes to both

[2] The residue numbering used here is that of the homologous *T. californica* acetylcholinesterase for which several X-ray structures exist. The catalytic triad in human acetylcholinesterase is Glu-334−His-447−Ser-203, and the nearby glutamate is Glu-202.

Scheme 1

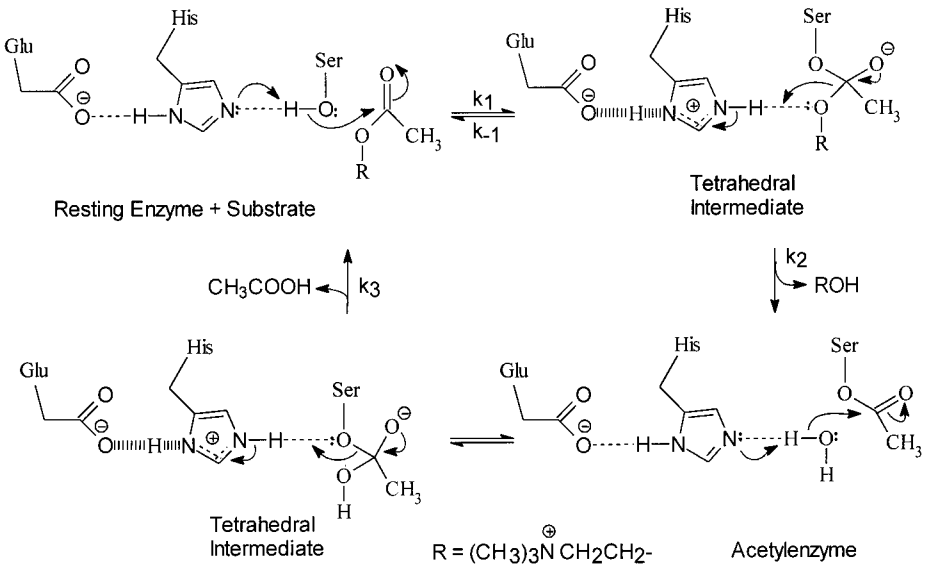

subsites. In addition, Glu-199 has been implicated in promoting the dealkylation of phosphonylated adducts of cholinesterases (*29*−*31*) and may also serve as a surrogate base catalyst in the hydrolysis of bulky substrates (*32*). Thus, it is possible that Glu-327 and Glu-199 can function as alternate hydrogen bond acceptors of the protonated His-440 donor in the active site of AChE.

Because of the critical role of AChE in neurotransmission and because of its high catalytic power, we have extended the use of ^{1}H NMR to recombinant human AChE, a 136 kDa homodimer (*33*), to determine whether SSHBs form at the active site, as we had previously found with equine BChE (*1*). With AChE, when a tetrahedral adduct was formed with the mechanism-based inhibitor TMTFA, a single, highly deshielded proton resonance with a low D/H fractionation factor was detected, indicating the formation of a SSHB between His-440 and Glu-327 of the catalytic triad.[2] When the pH is lowered to 5.1 with free, human AChE, or on formation of tetrahedral phosphate or phosphonate adducts of the active-site serine, *two* deshielded proton resonances were detected, the sum of which was approximately stoichiometric with the active-site concentration. We assign these two signals to SSHBs between slowly interconverting conformers of His-440 and the alternate acceptors, Glu-327 and Glu-199. This conformational heterogeneity of the active-site histidine was not observed with equine BChE in solution (*1*), or with *T. californica* AChE in the crystalline state (*20*−*23*), which show only *one* hydrogen-bonded species of the catalytic histidine under these conditions.

EXPERIMENTAL PROCEDURES

Materials. Anhydrous methanol, 2-propanol, tetrahydrofuran, diethyl ether, benzene, 3-bromoaniline, dimethyl sulfate, *tert*-butyllithium, ethyl trifluoroacetate, iodomethane, dichloromethylphosphonate, 4-nitrophenol, potassium carbonate, and deuterium oxide (D_2O, 99.96 at. % D) were purchased from Aldrich Chemical Co. Chelex-100 was from Bio-Rad. DTNB and ATC were from Sigma. All solvents and reagents were analytical or reagent grade and were used without further purification unless otherwise indicated. All buffer solutions used in the NMR experiments were treated with Chelex-100 resin to remove trace paramagnetic metals before addition to NMR samples.

Enzyme Preparation. Dimeric recombinant human AChE (EC 3.1.1.8) was prepared and assayed as described previously (*33*). The enzyme preparations were purified by two cycles of affinity chromatography on acridinium chloride resin to ≥95% homogeneity as determined by SDS−PAGE. The purity of the enzyme was confirmed by its specific activity (6000 units/mg of protein), where 1 unit represents the hydrolysis of 1 μmol of ATC per minute (*34*). The concentration of the enzyme was determined by its UV absorbance at 280 nm ($A_{1mg/mL}$ = 1.92). The enzyme preparations were preserved with decamethonium chloride until they were used for NMR studies, when they were dialyzed against 50 mM sodium phosphate buffer (pH 7.5) until essentially complete activity was recovered.

Mechanism-Based Inhibitors. TMTFA was prepared as described previously (*35*). The intermediate, *m*-(*N*,*N*-dimethylamino)trifluoroacetophenone, was purified by successive silica gel column chromatographies. The TMTFA product was further purified by repeated washing with dry ether and dried in vacuo at room temperature. Characterization by ^{1}H NMR confirmed the correct structure (*35*). Paraoxon was from Aldrich. The sarin analogue, 4-nitrophenyl-2-propyl methylphosphonate (NPMP), was synthesized as described previously (*36*) and purified by column chromatography on silica gel (70−230 mesh) eluting with a 20:1 chloroform/acetone mixture to 95% purity as determined by its boiling point, ^{1}H NMR spectrum, and hydrolysis to yield 4-nitrophenol.

General NMR Methods. Unless otherwise stated, 0.6 mL NMR samples contained 0.09 mM human AChE subunits in 50 mM sodium phosphate buffer (pH 7.5) and 10% (v/v) D_2O for field/frequency locking. When present, the mechanism-based inhibitors TMTFA, paraoxon, and NPMP were at 3-, 6-, and 4-fold molar excess, respectively, over the enzyme subunit concentration. The NMR data were collected on a Varian Unity Plus 600 MHz spectrometer using a Varian 5 mm triple-resonance probe at 25 °C. Data were processed on a Sun workstation operating the NMR spectrometer using the VNMR 6.1b software and/or on a Silicon Graphics

Indigo2 XZ workstation using the Felix 2.3 software package (Molecular Simulations Inc.). The 1:3:3:1 pulse sequence (*37*) was used to avoid water excitation. One-dimensional ^{1}H NMR data sets were collected as described previously (*14*) with the following modifications. The delays between the pulses were adjusted for a maximum excitation at 16.7 ppm (i.e., 12 ppm from the carrier which is positioned at H_2O), and the acquisition parameters included a 2.5 s relaxation delay, a 512 ms acquisition time, and a 30 μs 90° pulse width. A one-dimensional spectrum of free AChE at pH 7.5 was collected using 8000 transients. In addition, one-dimensional spectra of the free enzyme were also collected at pH 6.5, 5.7, and 5.1 using 24 000 transients**.** With TMTFA-treated enzyme samples, spectra were collected using 15 000 transients. With paraoxon-treated samples, spectra were collected 3, 5, 18, and 35 days after addition of the inhibitor to permit the slow deethylation of the Ser diethyl phosphate triester, using 5000, 23 000, 24 000, and 27 000 transients, respectively. All chemical shifts are reported with respect to external TSP, similarly locked on D_2O. To permit comparison of intensities of deshielded proton resonances in different spectra, the integrated area of each resonance was normalized to a methyl signal at −0.3 ppm in the same spectrum, the intensity of which was constant.

The D/H fractionation factor (ϕ) of a hydrogen-bonded site on an enzyme is defined as

$$\phi = [\text{Enz-D}][\text{H}_{\text{solvent}}]/[\text{Enz-H}][\text{D}_{\text{solvent}}] \qquad (1)$$

To measure the fractionation factors of the deshielded proton resonances at maximal sensitivity (*1*, *9*), the TMTFA−AChE sample was divided into two halves (0.050 mM final subunit concentration). To one half was added an H_2O solution of 50 mM sodium phosphate buffer (pH 7.5) containing 9.99% (v/v) deuterated D_2O, and to the other half was added an otherwise identical buffer solution in 99.9% (v/v) D_2O, resulting in samples with mole fractions of H_2O of 0.9004 and 0.5004, respectively. NMR spectra of the sample containing 0.9004 mole fraction H_2O (35 000 transients) were collected first, allowing the 0.5004 mole fraction H_2O sample to equilibrate at 4 °C for at least 48 h. Data on both samples were collected and processed identically. This identical procedure was used with the NPMP-modified sample, which had been aged for 17 days at 2 °C. The final NPMP-modified samples contained 0.040 mM enzyme subunits and 0.9004 and 0.5004 mole fraction H_2O. The fractionation factor (ϕ) was calculated by simultaneous equations of the form of eq 2, which is derived from eq 1.

$$I = [I_{\text{max}}(X)]/[\phi(1 - X) + X] \qquad (2)$$

where X is the mole fraction of H_2O, $1 - X$ is the mole fraction of D_2O, I is the observed peak intensity, and I_{max} is the maximal peak intensity at $X = 1.00$ (*14*).

Determination of the Lengths of the SSHBs in the AChE Adducts. Chemical shifts and fractionation factors provide precise and independent measurements of hydrogen bond lengths (*1*, *9*, *14*). A correlation of hydrogen bond distances (D) for 12 crystalline imidazolium−carboxylate interactions from small molecule, high-resolution X-ray diffraction, with chemical shifts of the protons in the hydrogen bonds (δ) obtained by solid-state NMR studies of the same crystals (*38*), was well fitted by the empirical relationship (*1*)

$$D = 1.99 + 0.198 \ln(\delta) + (10.14/\delta)^5 \qquad (3)$$

Equation 3 has been shown to yield precise measurements of hydrogen bond lengths in BChE (*1*) and in several serine proteases,[3] which agreed with those independently determined from the D/H fractionation factors of these protons, as well as with the less precise distances obtained by protein crystallography.

The fractionation factor (ϕ) measures the preference of a hydrogen-bonded site for deuterium over protium, relative to solvent (eq 1). As discussed in detail elsewhere (*9*, *14*), a hydrogen-bonded proton vibrates in one of two potential energy wells, each centered at one covalent bond length from the donor and acceptor heavy atoms. As the hydrogen bond becomes shorter, these wells approach each other, becoming broader and shallower. The latter effect decreases the zero-point vibrational energy of the hydrogen-bonded proton. Because of the 2-fold greater mass of a deuteron, its zero-point vibrational energy decreases $\sim(2)^{1/2}$-fold less, resulting in a decreased preference for deuterium over protium (ϕ) as the hydrogen bond shortens. Using quartic potential functions as proposed by Kreevoy and Liang (*39*), Bao et al. have derived a graph, which relates ϕ values to distances between the two proton wells (*6*). With this graph, we have determined distances between the two proton wells from measured ϕ values and have shown that precise hydrogen bond lengths can be obtained by adding two covalent bond lengths to this distance (*1*, *9*, *14*).

RESULTS AND DISCUSSION

Interaction of TMTFA with AChE. As found by X-ray studies (*21*), the mechanism-based inhibitor TMTFA forms a tetrahedral adduct of Ser-200 at the active site of AChE, analogous to the first tetrahedral intermediate formed with acetylcholine (Figure 1). The downfield region of the ^{1}H NMR spectrum of free AChE (0.09 mM subunits), in the presence of 45 mM sodium phosphate buffer (pH 7.5) and 10% D_2O, at 25 °C, showed a strong resonance at 14.4 ppm, 200 Hz in width, but no signals between 15 and 21 ppm (Figure 2A and Table 1). Addition of a 3-fold molar excess of TMTFA (0.27 mM) to the NMR sample resulted in the immediate and complete disappearance of the resonance at 14.4 ppm and the appearance of a highly deshielded resonance at 17.8 ppm, 170 Hz in width, with an integrated area that was 95 ± 10% of that of the 14.4 ppm resonance that had disappeared (Figure 2B and Table 1). This downfield resonance indicates the formation of a SSHB in the TMTFA adduct, which was confirmed by its low D/H fractionation factor (ϕ = 0.76 ± 0.10), determined as described in Experimental Procedures. This ϕ value is in good agreement with the transition state fractionation factors of 0.50−0.76 (error range of 2−7%) obtained from solvent isotope effects and proton inventory studies on $k_{\text{cat}}/K_{\text{m}}$ for the AChE-catalyzed hydrolysis of phenyl acetate (*40*), 4-nitrophenyl acetate (*41*), *o*-nitroacetanilides (*27*), and methyl acetate (*26*). Since acetylation is probably the dominant rate-determining step in these reactions at low substrate concentrations, the

[3] A. S. Mildvan and T. K. Harris, unpublished observations, 2000.

Table 1: NMR Properties of Hydrogen-Bonded Protons of Human Acetylcholinesterase at pH 7.5 and 25 °C

adduct	δ (ppm)	resonance width (Hz)	relative area[a]	$t_{1/2}$ of aging (days)	k_{ex} (s^{-1})	pK_a
none	14.4	200	1.00	−	<630	5.9 ± 0.3[b]
TMTFA	17.8	170	0.95 ± 0.10	<0.04	<530	−
paraoxon	15.5	164	0.56 ± 0.04	11 ± 2[c]	<515	−
	16.6	212	0.28 ± 0.02	11 ± 2[c]	<666	−
H^+ (pH 5.1)	16.4	280	0.94 ± 0.10	<0.04	<880	5.8 ± 0.3[d]
	17.7	280	0.30 ± 0.10	<0.04	<880	6.3 ± 0.2[b]
NPMP	15.8	109	0.46 ± 0.03	0.63 ± 0.28	<342	−
	16.5	144	0.51 ± 0.04	0.47 ± 0.13	<452	−

[a] The integrated areas of all deshielded resonances were normalized to a methyl resonance in the same spectrum, at −0.3 ppm, which did not change. [b] From the pH dependence of the integrated area. [c] At 2 °C. [d] From the pH dependence of the chemical shift, which increased by 2.0 ppm between pH 6.5 and 5.1.

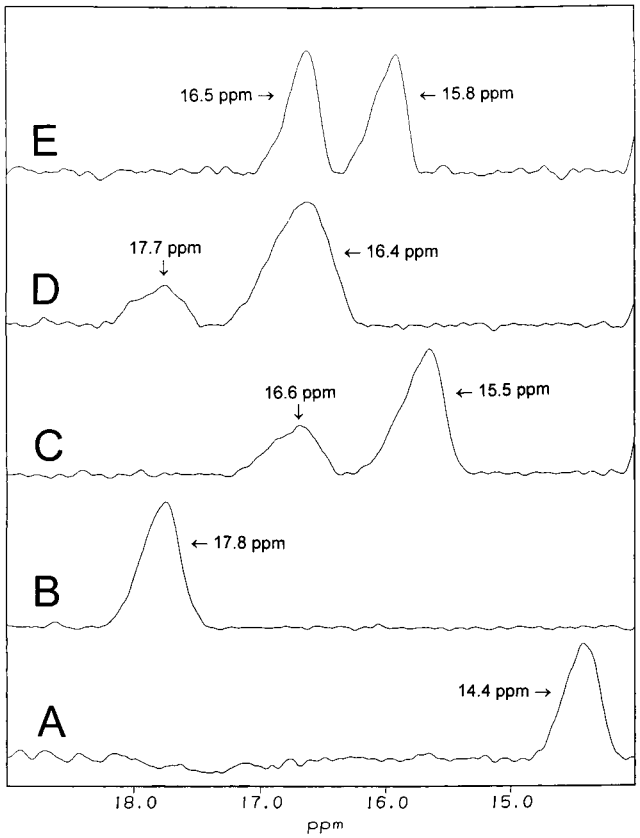

FIGURE 2: One-dimensional ^{1}H NMR spectra obtained by the 1:3:3:1 pulse sequence at 25 °C showing the downfield region (13.6−19.0 ppm) of solutions of human AChE (0.09 mM subunits). Other components were 45 mM sodium phosphate buffer (pH 7.5) and 10% D_2O. (A) Free AChE at pH 7.5 showing a resonance at 14.4 ppm assigned to neutral His-440 imidazole-NH. (B) AChE reacted with a 3-fold excess of TMTFA showing a resonance at 17.8 ppm. (C) AChE reacted with a 6-fold excess of paraoxon and fully dealkylated showing resonances at 15.5 and 16.6 ppm. (D) Free AChE at pH 5.1 showing resonances at 16.4 and 17.7 ppm. (E) AChE reacted with a 4-fold excess of NPMP and fully dealkylated showing resonances at 15.8 and 16.8 ppm. Note the disappearance of the 14.4 ppm resonance assigned to His-440 imidazole-NH in spectra B−E.

kinetically determined fractionation factors likely apply to the proton transferred from Ser-200 to the Nϵ of His-440.

The agreement of the NMR with kinetically determined ϕ values and the fact that the SSHB forms on binding the mechanism-based inhibitor TMTFA indicates that the SSHB is at the active site, very likely between His-440 NδH and Glu-327 Oϵ of the catalytic triad (Glu-327−His-440−Ser-200). The complete disappearance of the resonance at 14.4 ppm and its quantitative replacement with the signal at 17.8 ppm suggests its assignment to either the NδH or the NϵH of neutral His-440 in the free enzyme.

From eq 3, the chemical shift of 17.8 ± 0.05 ppm for the AChE−TMTFA adduct yields a hydrogen bond length of 2.62 ± 0.02 Å, taking into account the experimental error in δ (Table 2). Independently, the fractionation factor ϕ of 0.76 ± 0.10 yields a distance between the two proton wells of 0.63 ± 0.03 Å, taking into account the experimental error in ϕ. Adding two covalent bond lengths (2.00 Å) to this distance yields a hydrogen bond length of 2.63 ± 0.03 Å (Table 2). Such simple addition assumes the hydrogen bond is linear. If the hydrogen bond were bent, it would be even shorter (*9*, *14*). These NMR-derived distances agree with each other and with those found by NMR in the BChE−TMTFA complex [2.61 ± 0.03 Å (*1*)]. They also agree with the distance from His-440 Nδ to Glu-327 Oϵ in the X-ray structure of the TMTFA adduct of the homologous AChE from *T. californica*, 2.66 ± 0.28 Å (*21*) (Table 2 and Figure 1). However, the order of magnitude greater precision of the NMR-derived distances establishes the presence of a SSHB in the AChE−TMTFA complex, as was found in the BChE−TMTFA complex (*1*).

Interaction of Paraoxon with AChE. The mechanism-based inhibitor paraoxon initially phosphorylates the active-site Ser-200, with the departure of 4-nitrophenolate, and then slowly undergoes deethylation [$t_{1/2} \sim 41$ h at 37 °C (*42*)], yielding a serine ethyl phosphate diester anion, an analogue of the tetrahedral intermediate formed after water attack on the acyl enzyme (*1*, *28*). The addition of a 6-fold excess of paraoxon (0.54 mM) to a solution of AChE (0.09 mM subunits) containing 45 mM sodium phosphate buffer (pH 7.4), 10% D_2O, and 0.47% methanol at 25 °C resulted in the release of 4-nitrophenolate within minutes, and the rapid and complete disappearance of the resonance at 14.4 ppm, within the 2 h required to obtain an acceptable spectrum. This was followed by the very slow appearance ($t_{1/2} = 11 \pm 2$ days at 2 °C) of two deshielded resonances at 15.5 and 16.6 ppm with line widths of 164 and 212 Hz and relative integrated areas of 2 and 1, respectively (Figure 2C and Table 1). After 35 days of aging at 2 °C, the sum of the integrated areas of these deshielded signals corresponded to $84 \pm 10\%$ of the area of the 14.4 ppm signal that had disappeared, reflecting the nearly complete deethylation of the paraoxon adduct. The chemical shifts of 16.6 and 15.5 ppm yielded, from eq 3, hydrogen bond distances of 2.63 ± 0.02 and 2.65 ± 0.02 Å,

Table 2: Hydrogen Bond Distances at the Active Site of Human Acetylcholinesterase from NMR and X-ray Data

enzyme complex	δ^a (ppm)	ϕ	distance (Å) from δ	distance (Å) from ϕ	distance (Å) from X-ray
TMTFA	17.8	0.76 ± 0.10	2.62 ± 0.02	2.63 ± 0.03	2.66 ± 0.28[b]
paraoxon	15.5	−	2.65 ± 0.02	−	2.64 ± 0.22[c]
	16.6	−	2.63 ± 0.02	−	2.53 ± 0.24[d]
H^+ (pH 5.1)	16.4	−	2.63 ± 0.02	−	2.52 ± 0.25[e]
	17.7	−	2.62 ± 0.02	−	2.52 ± 0.25[e]
NPMP	15.8	0.49 ± 0.10	2.65 ± 0.02	2.56 ± 0.03	2.53 ± 0.26[f]
	16.5	0.47 ± 0.10	2.63 ± 0.02	2.55 ± 0.03	2.53 ± 0.26[f]

[a] Errors in δ are ±0.05 ppm. [b] AChE−TMTFA adduct (*21*). [c] AChE−VX adduct (*22*). [d] Aged AChE−VX adduct (*22*). [e] Free AChE at pH 5.8 (*21*). [f] Aged sarin adduct (*23*). The aged soman adduct, identical in structure, shows a distance of 2.60 ± 0.22 Å (*23*).

respectively (Table 2), indicating that both protons are in SSHBs. In contrast to the deethylated paraoxon adduct of AChE, the deethylated paraoxon adduct of BChE showed only a single downfield resonance at 16.1 ppm with a hydrogen bond length of 2.63 ± 0.04 Å, based on both its δ and ϕ values (*1*).

With AChE, the detection of two downfield resonances of unequal intensity, with the same half-time for appearance, is most simply explained by the presence of two unequally populated states of the SSHB in the serine ethyl phosphate diester anion. One state is very likely the hydrogen bond in the catalytic triad from His-440 NδH to Glu-327 Oϵ, as found in the X-ray structure of the aged, deethylated VX adduct of AChE, with a hydrogen bond length of 2.53 ± 0.24 Å (*22*). The other state may well involve a SSHB from His-440 NδH to Glu-199 Oϵ, another active-site residue as illustrated in Scheme 2. Such a hydrogen bond, 2.64 ± 0.22 Å in length, was found in the X-ray structure of the initial VX adduct of AChE, prior to its deethylation (*22*). Alternatively, both states of the SSHB could be between His-440 NδH and Glu-327 Oϵ, differing only in the hydrogen bond acceptor of the NϵH of His-440, which could be directed toward the bridging Ser-O-P in one state and to a nonbridging anionic phosphate oxygen in the other state. While evidence exists from neutron diffraction studies of DIFP-inhibited trypsin that His NϵH points to an anionic phosphate oxygen (*43*), and the X-ray structures of phosphorylated and dealkylated adducts of AChE also permit such a H-bond (*22*, *23*), this explanation is unlikely, since two similarly deshielded resonances are also seen in free AChE, without tetrahedral adducts, but at low pH where His-440 is protonated (see below). For this same reason, the existence of two environments for His-440 probably does not result from steric effects of the bulky adduct, but from the availability of Glu-199 at the active site. In contrast, in the AChE−TMTFA adduct, where Glu-199 approaches the quaternary nitrogen of the adduct and is therefore unavailable for hydrogen bonding (Figure 1), only one SSHB was observed, that between Glu-327 and His-440.

The NMR data with the ethyl phosphate derivative of AChE show that the longer hydrogen-bonded species predominate 2:1, and the two positions of His-440 interchange at a rate much slower than 666 s^{-1} at 25 °C on the basis of their resonance widths (Table 1). The slowness of this exchange of His-440 NδH between two acceptors (Glu-327 Oϵ and Glu-199 Oϵ) precludes the participation of this process in catalysis with acetylcholine, which occurs with a k_{cat} of 1.6 × 10^4 s^{-1} (*26*, *27*). However, this exchange may well contribute to the slow dealkylation of phosphorylated

Scheme 2

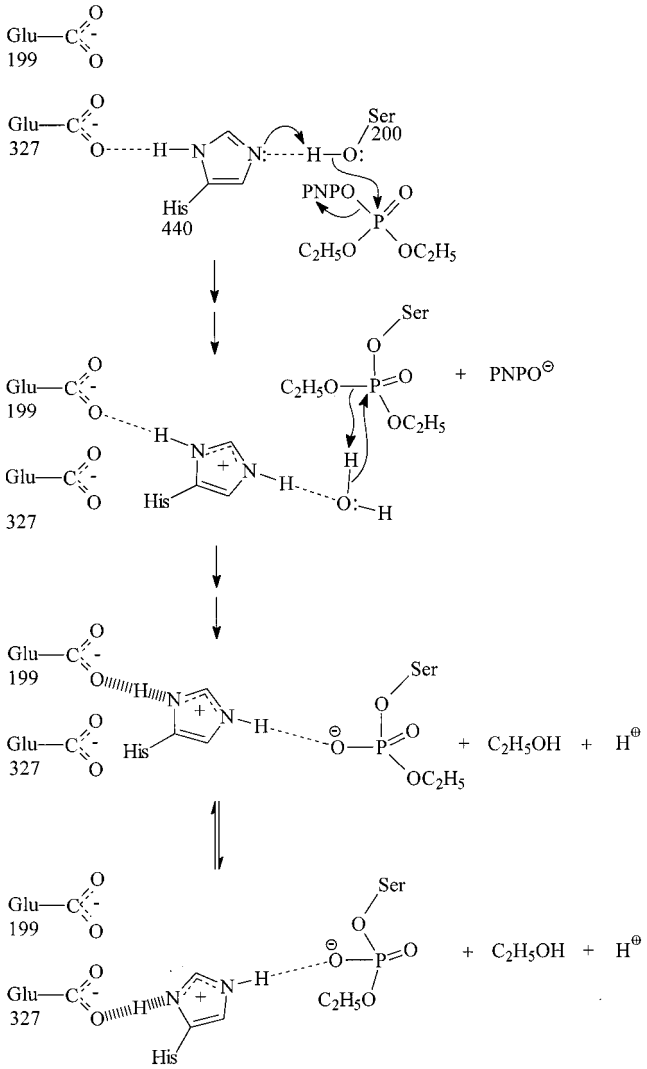

adducts of Ser-200, as suggested by the observation that the E199Q mutation of AChE is an order of magnitude more damaging to the rate of dealkylation than to k_{cat} (*44*−*47*). Moreover, the pH dependence of the rate of dealkylation of the soman adduct of AChE suggests the participation of two carboxylate groups (*12*, *46*, *47*), and molecular dynamics calculations suggest that Glu-199 is closer to His-440 in phosphonate adducts than in the tetrahedral intermediate formed during the hydrolysis of the acetyl enzyme (*10*, *11*, *13*).

The absence of deshielded proton resonances in the initial serine diethyl phosphate ester adduct may result from steric

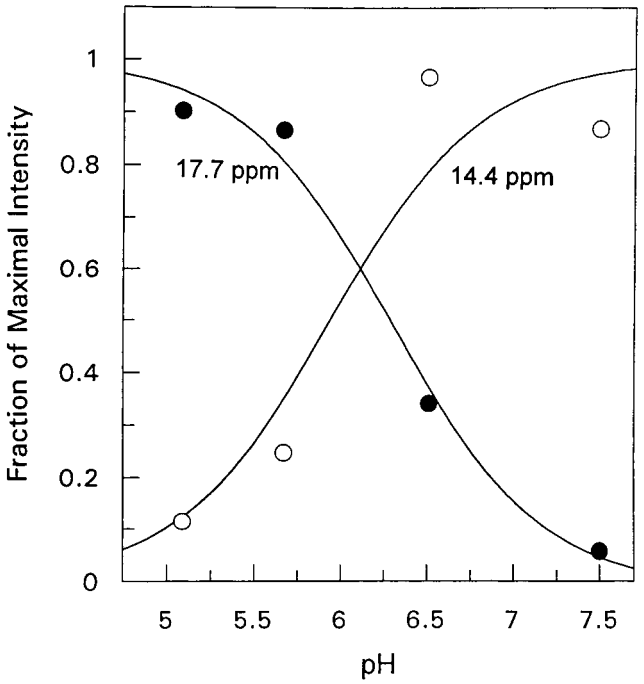

FIGURE 3: Effect of pH on the intensities of the deshielded proton resonances of free AChE. Components and conditions were as described in the legend of Figure 2. The pH was lowered by the addition of microliter amounts of 0.6 M HCl. The signals were integrated and normalized to the intensity of an unchanging methyl resonance of the enzyme at −0.3 ppm in the same spectra and expressed as the fraction of their respective maximal intensities. The maximal intensity of the 17.7 ppm resonance was 30 ± 10% of that of the 14.4 ppm resonance. The fitted titration curves were computed with pK_a values of 6.3 ± 0.2 and 5.9 ± 0.3 for the 17.7 and 14.4 ppm resonances, respectively.

distortion of the active site by the triester, which might weaken the hydrogen bonds from His-440 to both Glu-327 and Glu-199 shifting the NH resonances upfield to a position under the envelope of numerous other unresolved NH signals in this 136 kDa homodimer. Upon dealkylation, the distortion would be relieved, permitting the formation of SSHBs. Alternatively, the NH resonances may be undetected as a result of exchange broadening.

Effect of pH on the Deshielded Resonances of AChE. As described above, free AChE at pH 7.5 showed a strong resonance at 14.4 ppm (Figure 2A). A stepwise decrease in pH to 5.1 by microliter additions of 0.6 M HCl resulted in the progressive loss of intensity of this signal with an apparent pK_a of 5.9 ± 0.3, and the progressive appearance of a resonance at 17.7 ppm with a similar apparent pK_a of 6.3 ± 0.2, and with an intensity that was 30 ± 10% of that of the original signal at 14.4 ppm (Figure 3 and Table 1). In addition, at pH 5.1, a 3.2-fold stronger resonance appeared at 16.4 ppm with an intensity that was 94 ± 10% of that of the original signal (Figure 2D). The chemical shift of this resonance increased by 2.0 ppm with decreasing pH between pH 6.5 and 5.1, yielding an apparent pK_a of 5.8 ± 0.3 (Table 1). Separate experiments showed that these effects of pH are reversible. At pH 5.1, the sum of the intensities of the resonances at 17.7 and 16.4 ppm (124 ± 20%) is comparable to the intensity of the 14.4 ppm signal that disappeared. The widths of these two deshielded resonances (280 Hz) indicate exchange rates of $<880\ s^{-1}$ for both (Table 1). Thus, as found with serine proteases at low pH (*3*, *5*), protonation of His-440 in free AChE resulted in the formation of SSHBs involving this residue.

From the chemical shifts of 17.7 and 16.4 ppm, hydrogen bond lengths of 2.62 ± 0.02 and 2.63 ± 0.02 Å, respectively, are calculated with eq 3 (Table 2), in agreement with the distance of 2.52 ± 0.25 Å found between His-440 Nδ and Glu-327 Oϵ in the X-ray structure of free AChE at pH 5.8 (*20*). As with the deethylated paraoxon adduct (Figure 2C), the finding of two SSHBs in free human AChE at low pH (Figure 2D) indicates the presence of two slowly exchanging, unequally populated hydrogen bonding environments for cationic His-440. The failure of the X-ray structure of *T. californica* AChE at pH 5.8 to detect this conformational heterogeneity of His-440 may result from the species difference between the homologous enzymes from human and *T. californica*, or from the inability of the mixture of conformers to form suitable crystals.

Interaction of AChE with NPMP. To provide additional evidence that the detection of two deshielded resonances with the aged paraoxon adduct of AChE did not result from the slow and incomplete dealkylation of bound paraoxon, a different tetrahedral adduct which dealkylates much more rapidly was studied. The compound NPMP is a less volatile analogue of the nerve agent sarin. After initially phosphonylating the active-site serine of human AChE with the loss of 4-nitrophenolate, this adduct rapidly dealkylates, losing its isopropyl group with a $t_{1/2}$ of 3.3 h at 37 °C (*48*), a rate 12.4-fold greater than the rate of deethylation of the paraoxon adduct of human AChE at the same temperature and pH (*42*), leaving a methylphosphonate ester anion of Ser-200.

The addition of a 4-fold excess of NPMP (0.4 mM) to an NMR sample containing human AChE (0.09 mM subunits) in the presence of 45 mM sodium phosphate (pH 7.5), 80 mM NaCl, and 10% D_2O resulted in the rapid appearance of free 4-nitrophenol within seconds, and the rapid disappearance of the His-440 resonance at 14.4 ppm, well within the 3 h required to obtain an acceptable spectrum. This was followed by the slower and simultaneous appearance of two deshielded proton resonances at 16.5 and 15.8 ppm (Figure 2E and Table 1). The average half-time for appearance of both signals was 13.2 ± 5.7 h at 25 °C (Table 1), in good agreement with a previous measurement,[4] which was 20 ± 9-fold faster than the rate of deethylation of the paraoxon adduct (at 2 °C), as measured by the appearance of its downfield resonances (Table 1). These relative rates of dealkylation of the NPMP and paraoxon adducts are comparable to literature values measured at 37 °C (*42*, *48*). The widths of the resonances at 16.5 and 15.8 ppm in the aged NPMP adduct were 144 and 109 Hz, respectively, and their integrated areas were approximately equal, with an intensity ratio of 1.10 ± 0.10 for the 16.5 ppm/15.8 ppm resonances (Table 1). Their total integrated area, after 3.4 half-times, was 97 ± 10% of the initial 14.4 ppm resonance of His-440 that had disappeared, indicating essentially stoichiometric phosphonylation of the active-site serine and dealkylation.

The chemical shifts of these resonances at 16.5 and 15.8 ppm yielded, from eq 3, hydrogen bond lengths of 2.63 ± 0.02 and 2.65 ± 0.02 Å respectively, consistent with two slowly exchanging, equally populated SSHBs in the dealky-

[4] I. M. Kovach, unpublished data, 1990.

lated methylphosphonate ester of the active-site serine in AChE. The low fractionation factors of these resonances (Table 2) confirm the presence of SSHBs, yielding slightly shorter distances of 2.55 ± 0.03 and 2.56 ± 0.03 Å, respectively. The fractionation factors of 0.47−0.49 ± 0.10 obtained by NMR (Table 2) overlap with those obtained for k_{cat}, which is determined partially by acetylation and partially by deacetylation in the AChE-catalyzed hydrolysis of phenyl acetate (ϕ = 0.413 ± 0.004) (*40*), *o*-nitroformanilide and *o*-nitroacetanilides (ϕ = 0.541−0.571) (*27*), and 4-methoxyphenyl formate (ϕ = 0.38 ± 0.02) (*27*), although the kinetically determined fractionation factors likely involve proton transfer to His-440 Nϵ from Ser-100 in acetylation, and from water in deacetylation. These similarities in ϕ suggest that the methylphosphonate ester anion of the catalytic serine mimics the quasi-tetrahedral transition states in the formation and hydrolysis of the acetyl enzyme (Scheme 1). The X-ray structures of the aged AChE adducts of both sarin and soman (*23*) show identical methylphosphonate esters of Ser-200 with hydrogen bond lengths from His-440 Nδ to Glu-327 Oϵ of the catalytic triad of 2.53 ± 0.26 and 2.60 ± 0.22 Å, respectively (Table 2), suggesting that one of the two SSHBs detected by NMR results from the His-440−Glu-327 interaction. It is very likely that His is cationic under these conditions, since its pK_a is estimated to be 8.3 in the dealkylated soman adduct of BChE (*49*).

As proposed above for the deethylated paraoxon adduct, the additional SSHB detected by NMR may result from hydrogen bond donation by His-440 NδH to Glu-199 Oϵ, which is nearby. However, in the X-ray structure of the aged sarin adduct, only the above-mentioned hydrogen bond from His-440 Nδ to Glu-327 Oϵ is seen, and the nearest carboxylate oxygen of Glu-199 is 3.62 ± 0.26 Å from His-440 Nδ and 3.39 ± 0.26 Å from His-440 Nϵ. Similar distances, within these experimental errors, are found in the essentially identical X-ray structure of the aged soman adduct (*23*), providing no crystallographic evidence for the additional SSHB involving His-440 which is detected by NMR. As noted above, the failure to detect a second SSHB by X-ray may be a result of species differences between homologous AChEs from human and *T. californica*, or because the mixture of conformers may not form suitable crystals.

CONCLUSIONS

As previously found with equine BChE (*1*), human AChE forms SSHBs upon binding mechanism-based inhibitors which form tetrahedral adducts of the active-site serine analogous to the tetrahedral intermediates in catalysis, or at low pH, when the active-site histidine becomes protonated. The TMTFA adduct showed the simplest behavior, forming a single SSHB, 2.62 ± 0.03 Å in length, between His-440 Nδ and Glu-327 Oϵ of the Glu−His−Ser catalytic triad, in an amount stoichiometric with the neutral His-440 that was lost. Formation of the serine ethyl phosphate diester with paraoxon or the serine methylphosphonate monoester with NPMP resulted in the appearance of *two* slowly exchanging SSHBs, the total concentrations of which were approximately stoichiometric with the neutral His-440 that was lost. Similarly, two slowly exchanging SSHBs were seen with free AChE at pH 5.1 where His-440 is protonated with an apparent pK_a of 6.0 ± 0.4. The two SSHBs likely result from the slow interchange of His-440 NδH between two acceptors, Glu-327 of the catalytic triad, and the nearby residue, Glu-199. This conformational heterogeneity of His-440, readily detected by NMR, is not seen in the X-ray structures of the phosphorylated or phosphonylated adducts of the homologous AChE from *T. californica* or in the protonated form of this enzyme, either due to the species difference or because the mixtures of conformers did not form suitable crystals. The formation of a SSHB between Glu and His of the catalytic triad in the reaction mechanism (Scheme 1) would facilitate the deprotonation of Ser in the acylation reaction, and the deprotonation of the attacking water in the deacylation reaction, thus contributing to the high catalytic power of cholinesterases.

REFERENCES

1. Viragh, C., Harris, T. K., Reddy, P. M., Massiah, M. A., Mildvan, A. S., and Kovach, I. M. (2000) *Biochemistry 39*, 16200−16205.
2. Robillard, G., and Shulman, R. G. (1974) *J. Mol. Biol. 86*, 519−540.
3. Cassidy, C. S., Lin, J., and Frey, P. A. (1997) *Biochemistry 36*, 4576−4584.
4. Tobin, J. B., Whitt, S. A., Cassidy, C. S., and Frey, P. A. (1995) *Biochemistry 34*, 6919−6924.
5. Lin, J., Westler, W. M., Cleland, W. W., Markley, J. L., and Frey, P. A. (1998) *Proc. Natl. Acad. Sci. U.S.A. 95*, 14664−14668.
6. Bao, D., Huskey, W. P., Kettner, C. A., and Jordan, F. (1999) *J. Am. Chem. Soc. 121*, 4684−4689.
7. Golubev, N. S., Denisov, G. S., Gindin, V. A., Ligay, S. S., Limbach, H.-H., and Smirnov, S. N. (1994) *J. Mol. Struct. 322*, 83−91.
8. Halkides, C. J., Wu, Y. Q., and Murray, C. J. (1996) *Biochemistry 35*, 15941−15948.
9. Harris, T. K., and Mildvan, A. S. (1999) *Proteins: Struct., Funct., Genet. 35*, 275−282.
10. Bencsura, A., Enyedy, I., and Kovach, I. M. (1995) *Biochemistry 34*, 8989−8999.
11. Bencsura, A., Enyedy, I., and Kovach, I. M. (1996) *J. Am. Chem. Soc. 118*, 8531−8541.
12. Kovach, I. M. (1998) in *Structure and Function of Cholinesterases and Related Proteins* (Doctor, B. P., Taylor, P., Quinn, D. M., Rotundo, R. L., and Gentry, M. K., Eds.) pp 339−344, Plenum Press, New York.
13. Enyedy, I. J., Kovach, I. M., and Bencsura, A. (2001) *Biochem. J. 353*, 645−653.
14. Mildvan, A. S., Harris, T. K., and Abeygunawardana, C. (1999) *Methods Enzymol. 308*, 219−245.
15. Zhao, Q., Abeygunawardana, C., Talalay, P., and Mildvan, A. S. (1996) *Proc. Natl. Acad. Sci. U.S.A. 93*, 8220−8224.
16. Zhao, Q., Abeygunawardana, C., Gittis, A. G., and Mildvan, A. S. (1997) *Biochemistry 36*, 14616−14626.
17. Harris, T. K., Abeygunawardana, C., and Mildvan, A. S. (1997) *Biochemistry 36*, 14661−14675.
18. Harris, T. K., Marks, G. T., Massiah, M. A., Mildvan, A. S., and Harrison, D. H. T. (2000) 220th National Meeting of the American Chemical Society, Washington, DC, August 20−24, 2000, Abstract 507.
19. Lipscomb, W. N. (1980) in *Methods for Determining Metal Ion Environments in Proteins* (Darnall, D. W., and Wilkins, R. G., Eds.) pp 265−302, Elsevier, New York.
20. Sussman, J. L., Harel, M., Frolow, F., Oefner, C., Goldman, A., Toker, L., and Silman, I. (1991) *Science 253*, 872−879.
21. Harel, M., Quinn, D. M., Nair, H. K., Silman, I., and Sussman, J. L. (1996) *J. Am. Chem. Soc. 118*, 2340−2346.
22. Millard, C. B., Koellner, G., Ordentlich, A., Shafferman, A., Silman, I., and Sussman, J. L. (1999) *J. Am. Chem. Soc. 121*, 9883−9884.
23. Millard, C. B., Kryger, G., Ordentlich, A., Greenblatt, H. M., Harel, M., Raves, M. L., Segall, Y., Barak, D., Shafferman,

A., Silman, I., and Sussman, J. L. (1999) *Biochemistry 38*, 7032−7039.
24. Brill, V. R., and Tippe, A. (1967) *Acta Crystallogr. 23*, 343−345.
25. Enyedy, I. J., Kovach, I. M., and Brooks, B. R. (1998) *J. Am. Chem. Soc. 120*, 8043−8050.
26. Rosenberry, T. L. (1975) *Adv. Enzymol. 43*, 104−218.
27. Quinn, D. M. (1987) *Chem. Rev. 87*, 955−975.
28. Kovach, I. M. (1988) *J. Enzyme Inhib. 2*, 199−208.
29. Qian, N., and Kovach, I. M. (1993) *FEBS Lett. 336*, 263−266.
30. Qian, N. F., and Kovach, I. M. (1993) *Med. Def. Biosci. Rev. 3*, 1005−1014.
31. Taylor, P., and Radic, Z. (1994) *Annu. Rev. Pharmacol. Toxicol. 34*, 281−320.
32. Selwood, T., Feaster, S. R., States, M. J., Pryor, A. N., and Quinn, D. M. (1993) *J. Am. Chem. Soc. 115*, 10477−10482.
33. Mallender, W. D., Szegletes, T., and Rosenberry, T. L. (1999) *J. Biol. Chem. 274*, 8491−8499.
34. Rosenberry, T. L., and Scoggin, D. M. (1984) *J. Biol. Chem. 259*, 5643−5652.
35. Nair, H. K., Lee, K., and Quinn, D. M. (1993) *J. Am. Chem. Soc. 115*, 9939−9941.
36. Bennet, A., Kovach, I. M., and Schowen, R. L. (1988) *J. Am. Chem. Soc. 110*, 7892−7893.
37. Turner, D. L. (1983) *J. Magn. Reson. 52*, 157−170.
38. Wei, Y., and McDermott, A. E. (1999) in *Modeling NMR Chemical Shifts: Gaining Insights into Structure and Environment* (Facelli, J. C., and de Dios, A. C., Eds.) pp 177−193, Oxford University Press, Cary, NC.
39. Kreevoy, M. M., and Liang, T. M. (1980) *J. Am. Chem. Soc. 102*, 3315−3322.
40. Kovach, I. M., Larson, M., and Schowen, R. L. (1986) *J. Am. Chem. Soc. 108*, 3054−3056.
41. Hogg, J. L., Elrod, J. P., and Schowen, R. L. (1980) *J. Am. Chem. Soc. 102*, 2082−2086.
42. Hobbiger, F. (1956) *Br. J. Pharm. 11*, 295−303.
43. Kossiakoff, A. A., and Spencer, S. A. (1981) *Biochemistry 20*, 6462−6474.
44. Saxena, A., Doctor, B. P., Maxwell, D. M., Lenz, D. E., Radic, Z., and Taylor, P. (1993) *Biochem. Biophys. Res. Commun. 197*, 343−349.
45. Ordentlich, A., Kronman, C., Barak, D., Stein, D., Ariel, N., Marcus, D., Velan, B., and Shafferman, A. (1993) *FEBS Lett. 334*, 215−220.
46. Viragh, C., Akhmetshin, R., Kovach, I. M., and Broomfield, C. (1997) *Biochemistry 36*, 8243−8252.
47. Saxena, A., Viragh, C., Frazier, D. S., Kovach, I. M., Maxwell, D. M., Lockridge, O., and Doctor, B. P. (1998) *Biochemistry 37*, 15086−15096.
48. Kovach, I. M., and Bennet, A. J. (1990) *Phosphorus, Sulfur Silicon Relat. Elem. 51/52*, 51−56.
49. Masson, P., Clery, C., Guerra, P., Redslob, A., Albaret, C., and Fortier, P. L. (1999) *Biochem. J. 343*, 361−369.

BI010243J